Blazars Studied with the *Suzaku* X-ray Telescope

Łukasz Stawarz[1, 2]

[1] ISAS/JAXA, 3-1-1 Yoshinodai, Chuo-ku, Sagamihara, Kanagawa 252-5210, Japan
[2] Astronomical Observatory, Jagiellonian University, ul. Orla 171, 30-244 Kraków, Poland
E-mail(LS): stawarz@astro.isas.jaxa.jp

Abstract

Blazars, which are radio-loud active galaxies with luminous jets aligned at small angles to the line of sight, form a rather heterogeneous population of extragalactic sources of high energy radiation. Frequently monitored over the last decades with different instruments ranging from low-frequency radio interferometers up to high and very high energy γ-ray telescopes, they enable a unique insight into the innermost parts of active galactic nuclei (AGN) where relativistic jets are launched by supermassive black holes accreting at high rates. The radiative output of blazars is however dominated by a non-thermal emission of high-energy jet particles, and hence extracting the key parameters of these systems requires a good understanding of particle acceleration processes taking place in relativistic collisionless plasma. Here I discuss some selected recent observational results on the topic obtained in the X-ray domain using the *Suzaku* satellite, which provides detailed broad-band spectra of blazar sources in relatively short (or very short) exposures. Such good-quality spectra are necessary for a precise characterization of the jet variability and energetics. I also comment on the prospects for the X-ray polarimetry of blazar sources with the Soft Gamma-ray Detector onboard the ASTRO-H satellite to be launched in 2015.

Key words: radiation mechanisms: non-thermal — acceleration of particles — galaxies: active — galaxies: jets — X-rays: galaxies

1. Introduction

Blazars are sources of non-thermal emission extending over many decades of the electromagnetic spectrum, from radio domain up to γ-rays. They are highly variable emitters, exhibiting a low-amplitude flickering along with orders-of-magnitude flares on various timescales ranging from minutes to years and decades. Blazars are divided into Flat Spectrum Radio Quasars (FSRQs) and BL Lacertae objects (BL Lacs) based on the optical emission lines properties (see Urry & Padovani 1995). For the recent review on various aspects of the blazar phenomenon see, e.g., Ghisellini (2013).

The broad-band spectra of blazars consist of two distinct components in the $\nu - \nu L_\nu$ representation. The low-energy one peaks in the infrared in the case of FSRQs, and at optical–to–X-ray frequencies in the case of BL Lacs. This component is due to the synchrotron emission of ultra-relativistic jet electrons, as evidenced by the detected radio and optical polarization. The high-energy component, peaking in γ-rays, is now most widely believed to be due to the inverse-Compton emission of the same electron population (Marscher & Gear 1985, Dermer & Schlickeiser 1993, Sikora et al. 1994). The alternative hadronic blazar emission models are now much less discussed than in the past, as they are seriously challenged by the refined energetic and spectral constraints (see the discussion in Sikora et al. 2009, 2013).

The location and structure of the blazar emission zone in the framework of the leptonic emission scenario, along with the particle acceleration processes involved, are the most widely debated open problems in blazar physics. The standard blazar paradigm established in the EGRET era consists of a conical, matter-dominated jet expanding with constant bulk Lorentz factor $\Gamma_j \sim 10$ and constant opening angle $\theta_j \sim 1/\Gamma_j$, which dissipates roughly $\sim 1\%$ of its bulk kinetic energy to the high-energy emission via internal shocks formed within the outflow at distances $r \sim \Gamma_j^2 r_g \ll 1\,\mathrm{pc}$ from the jet base, i.e. from approximately the event horizon $r_g = GM_{\rm BH}/c^2$ of a supermassive black hole residing in the center of an AGN. More recently, blazar emission models became however much more complex, and various authors consider strongly magnetized outflows containing large-scale organized magnetic field, gradually collimating and accelerating over several decades of spatial scales, surrounded by prominent shear layers, and dissipating a substantial fraction of their kinetic energies in ultra-compact emission sites via relativistic reconnection, magnetic turbulence, or reconfinement nozzles formed at larger distances from the jet base ($r \geq 1\,\mathrm{pc}$).

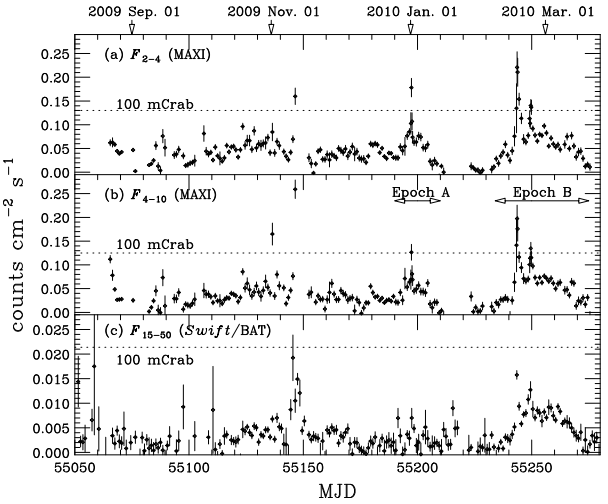

Fig. 1. Daily lightcurve of Mrk 421 from 2009 August 22 (MJD = 55062) to 2010 March 20 (MJD = 55275), represented as the normalized count rates in the 2–4 keV and 4–10 keV ranges measured with the MAXI GSC, and in the 15–50 keV range measured with *Swift*-BAT. All the errors represent the 1σ statistical uncertainity. The dotted lines indicate the count rate of 100 mCrab in the individual energy ranges. *(from Isobe et al. 2010.)*

Any comprehensive insight into the blazar phenomenon requires therefore an extensive set of good-quality data gathered at different frequencies, for a larger number of sources, during distinct activity states. But there are important limitations in each frequency domain available to modern telescopes. For example, blazar emission continua at lower radio frequencies are due to a superposition of self-absorbed spectra of different parts of the jets (Blandford & Koenigl 1979), and as such do not carry any direct information about the blazar emission zone. In the infrared–to–UV range, the total radiative output of blazar sources is often contributed significantly by the emission of dusty AGN tori, host galaxies, and accretion disks. The γ-ray segments of the blazar jet spectra, on the other hand, may be strongly modified by the photon-photon annihilation processes and the related pair cascades, both intrinsic to the blazar emission zone and in the intergalactic space (e.g., Poutanen & Stern 2010, Ackermann et al. 2012). For this reasons, the X-ray domain is in fact particularly well-suited for the blazar studies, as it is relatively free from absorption effects or a contribution from other (thermal) emission components.

2. Blazars Studied in X-rays

The all-sky X-ray monitors are very important in the blazar studies, since, as noted above, blazars are known to be erratic, highly variable emitters. Yet those instruments, especially the hard X-ray ones such as MAXI or *Swift*-BAT, are of a limited sensitivity, and hence uninterrupted X-ray lightcurves with good spectral constraints are restricted to only a few the X-ray brightest blazar sources, such as for example Mrk 421 (see Figure 1). The good-quality X-ray spectra for the majority of blazars have to be therefore provided by the high-sensitivity pointing satellites. Of those, the X-ray Observatory *Suzaku* (Mitsuda et al. 2007) has the particularly relevant capability of broad-band blazar observations, owing to the excellent sensitivity of its instruments X-ray Imaging Spectrometer (XIS; Koyama et al. 2007) in the 0.3–12 keV band, and the Hard X-ray Detector (HXD; Takahashi et al. 2007; Kokubun et al. 2007) in the 10–300 keV band.

2.1. BL Lacs

BL Lacs are relatively low-power but nearby sources, characterized by moderate and lower accretion rates ($\leq 1\%$ in the Eddington units; see, e.g., Sbarrato et al. 2012). Their X-ray spectra are typically dominated by the high-energy tails of the synchrotron continua, produced by the $E_e \geq 1$ TeV energy jet electrons. The long-term X-ray monitoring of BL Lacs revealed the red-noise type of flux changes with the characteristic variability timescales of the order of days, and the variability amplitudes depending on the flux level and photon energy (e.g., Kataoka et al. 2001). The established correlated variability in the X-ray and TeV bands in the brightest objects such as Mrk 421 (e.g., Takahashi et al. 2000, Fossati et al. 2008), was historically the crucial observational evidence for the inverse-Compton origin of the observed γ-ray emission of this class of AGN. *Suzaku* observations of BL Lacs targeted therefore predominantly the TeV-detected sources during the organized multiwavelength campaigns (e.g., Tagliaferri et al. 2008, Reimer et al. 2008, Anderhub et al. 2009).

Ushio et al. (2009) have utilized extensively the capability of the *Suzaku* instruments by constructing high-photon-statistics time-resolved 0.6–60 keV spectra of Mrk 421 for exposure times as short as a few ksec. These were analyzed by the parametric forward-fitting `SYNCHROTRON` model implemented in `XSPEC` (Tanaka et al. 2008), in which the X-ray data were fitted with synchrotron spectra originating from a given parameterized shape of the electron energy distribution, rather than with the assumed parametrized spectral form of the non-thermal emission continuum. Ushio et al. (2009) separate the observed spectra into the "steady" and "variable" components by subtracting the spectrum in the lowest- flux period from those of other data segments, and demonstrated that the steady emission component is best described by a synchrotron emission of the power-law electron energy distribution with the exponential cut-off; the variable emission component occurred instead to be best fitted with the broken power-law emission model (see Figure 2). The authors concluded that

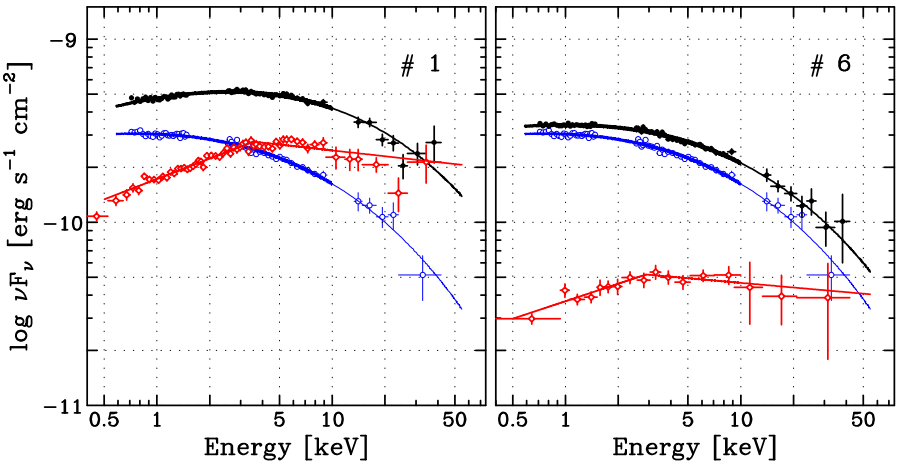

Fig. 2. Simultaneous X-ray spectra of "variable" and "stead" X-ray emission components in Mrk 421 corresponding to the high flux period (epoch No. 1, left panel) and the end of the decay period (epoch No. 6, right panel) during the *Suzaku* 2006 April campaign. The red and black data sets are for the "variable" components and the total (="steady"+"variable") spectra; the blue data set corresponds to the lowest-flux period and is common to two plots. *(from Ushio et al. 2009.)*

the rapidly variable component is most likely due to localized shock acceleration, while the slowly variable (steady) component is due to a superposition of shocks located at larger distance along the jet, or due to the stochastic acceleration on magnetic turbulence.

Ushio et al. (2010) extended this analysis by including also the simultaneous UV data for the target. They confirmed that the high-energy tail of the synchrotron emission continuum of Mrk 421 during the source quiescence is best fitted with the power-law electron energy distribution moderated by the exponential cutoff, and that the alternative, smoothly curved electron spectra, such as the log-parabolic one (often invoked in modeling the X-ray spectra of BL Lacs; see, e.g., Tramacere et al. 2009, and references therein), or ultra-relativistic Maxwellians (see Stawarz & Petrosian 2008), are not strictly required by the data. These results are of a particular relevance for the scenarios assuming the dominant role of the stochastic acceleration in blazar sources, in which smoothly curved electron spectra may be naturally expected (e.g., Katarzynski et al. 2006, Boutelier et al. 2008, Cao & Wang 2013, Asano et al. 2014).

Among the TeV-detected BL Lacs, the class of 'extreme high-frequency peaked' objects is especially interesting in the context of the X-ray observations, as the X-ray synchrotron continua of those sources extend up to hard X-rays even during quiescence states. The extreme BL Lacs seem peculiar for their physical properties, namely for particularly low magnetization but high bulk velocities of the emitting regions, as well as very high *minimum* electron energies (see Tavecchio et al. 2010). They may be relevant in the cosmological context as well, providing meaningful limits on the intergalactic magnetic field through a detailed modeling of their broad-band spectra allowing to put constraints on the cascade component arising from the absorption and re-procession of the γ-ray photons on the extragalactic background light (Neronov & Vovk 2010; Tavecchio et al. 2011; Dermer et al. 2011).

The candidate for the most extreme member of this class, HESS J1943+213, characterized by the hard X-ray spectrum with no apparent cut-off up to 195 keV photon energies as hinted by a long accumulation of the *Swift*-BAT data, was recently observed with *Suzaku* (Tanaka et al. 2014; see Figure 3). The observations revealed a steady X-ray continuum with the precisely constrained photon index $\Gamma_{0.5-25\,\mathrm{keV}} = 2.00 \pm 0.02$, implying the action of persistent and very efficient yet unspecified energy dissipation processes, accelerating jet electrons up to the highest accessible energies $E_e > 10$ TeV. The broad-band modeling of the source (based on Finke et al. 2008) confirmed the extremely low jet magnetic field $B' \sim 1$ mG, and high minimum electron Lorentz factor $\gamma_{\mathrm{min}} \sim 10^5$.

2.2. Flat Spectrum Radio Quasars

FSRQs are typically very luminous but distant objects. They are characterized by high accretion rates ($\geq 1\%$ in the Eddington units; see, e.g., Sbarrato et al. 2012), powerful jets, and total radiative outputs corresponding to the isotropic luminosities of the order of even $L_{\mathrm{iso}} \sim 10^{49}\,\mathrm{erg\,s^{-1}}$ during high-activity states. The X-ray spectra of FSRQs, believed to be dominated by the inverse-Compton emission of the lowest-energy jet electrons, are flat and often even very flat (photon indices $\Gamma_{\mathrm{X}} < 1.5$; see Sikora et al. 2009 and references therein). The X-ray variability of this class of blazars is rarely correlated with the radio, optical, or even high-energy γ-ray flux changes (see in this context, e.g., Hayashida et al.

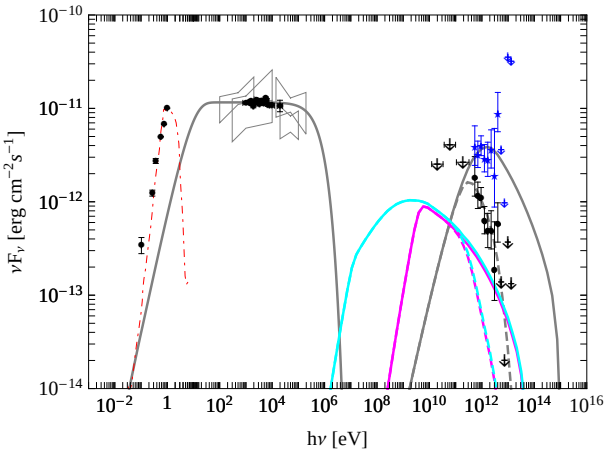

Fig. 3. Broadband spectral energy distribution of HESS J1943+213. Black filled circles/large arrows correspond to the non-simultaneous fluxes/upper limits, including the newly obtained *Suzaku* (re-binned XIS0+PIN) data; gray bowties denote the archival X-ray spectra of the source. Blue stars and small arrows denote the de-absorbed γ-ray spectrum, assuming a source distance of 600 Mpc. Various model curves represent different emission components calculated in the framework of the blazar fit, including synchrotron and synchrotron self-Compton ones (gray curves), along with the cascade spectra calculated for the intergalactic magnetic field of 10^{-16} G (magenta curves) and 10^{-18} G (cyan curves); the dashed curves denote the spectra with the γ-ray flux attenuation included; thin red dot-dashed curve illustrates the starlight of a giant elliptical galaxy located at a distance of 600 Mpc. *(from Tanaka et al. 2014.)*

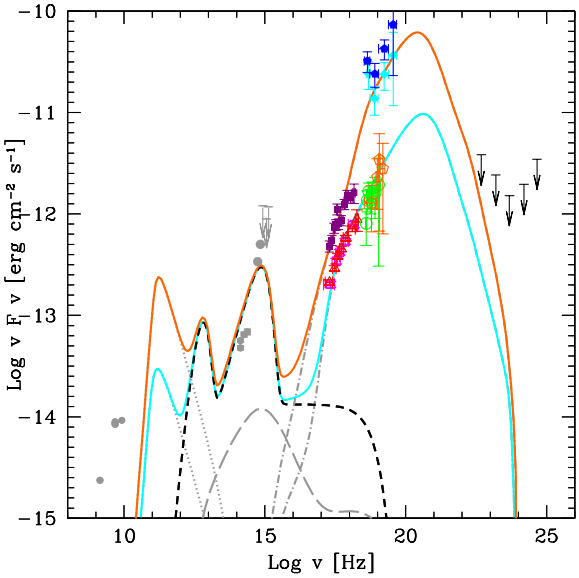

Fig. 4. Spectral energy distribution of IGR J22517+2217 ($z = 3.7$). Gray circles and arrows represent archival data from NED. Color symbol correspond to high-energy data gathered with different instruments, including *Suzaku* XIS 0 and XIS 3 (red triangles and magenta squares). Different curves denote the applied blazar model (quiescent and flaring states), along with the thermal emission components of the accretion disk, the dusty torus, and the Xray disk corona. *(from Lanzuisi et al. 2012.)*

2012). It should be noted that the X-ray domain is particularly useful in studying the highest-redshift FSRQs, which are relatively dim at frequencies other than hard X-rays/soft γ-rays (e.g., Watanabe et al. 2009, Ghisellini et al. 2010, Lanzuisi et al. 2012; see Figure 4).

The fact that the X-ray continua of FSRQs are, as noted above, flat within the broad energy range from below keV up to hundreds of keV, has several important implication for constraining the blazar emission models, content, and energetics (Sikora et al. 2009, 2013). An important point to make in this context is that the bulk of the kinetic power stored in jet electrons is expected to be carried by the lowest-energy particles, down to the mildly-relativistic regime. A large amount of such mildly-relativistic leptons, sufficient to account for the total jet kinetic luminosity, should however manifest as a distinct steep-spectrum component/bump in soft X-rays, due to the bulk-Comptonization of the UV accretion disk photons (e.g., Sikora & Madejski 2000, Moderski et al. 2004, Celotti et al. 2007). Hence, detections or even upper limits for such an emission component in the spectra of FSRQs were recognized already early on as very meaningful.

Dedicated *Suzaku* observations of the bright FSRQ PKS 1510–089, in search of the bulk-Compton spectral features, have been analyzed in detail by Kataoka et al. (2008). The obtained high signal-to-noise ratio X-ray spectrum of the source revealed an extremely hard power-law component with the photon index of $\Gamma_X \approx 1.2$, augmented by a soft component apparent below 1 keV and well described by a blackbody model with a temperature of $kT \approx 0.2$ keV (see Figure 5). The modeling of the detected soft X-ray excess in the framework of the bulk-Compton scenario indicated that the power of the jet is dominated by "cold" (mildly-relativistic) protons, but with a number of electrons and/or positrons exceeding the number of protons by a factor of ~ 10. The bulk-Compton interpretation of the soft X-ray feature is however not a unique one, as discussed in Kataoka et al. (2008). Still, even if the revealed excess does not correspond to the detection of the bulk-Compton component, but only provides the upper limit for such, the main conclusion stating that leptons are not numerous enough to carry the total jet kinetic power in the PKS 1510–089 jet, remains valid. The analogous analysis performed for the number of other FSRQs confirmed this result, excluding in particular the case of particle-dominated purely leptonic content, and therefore implying either a significant amount of protons in blazar jets, or Poynting flux-dominated outflows (see in this context Celotti & Ghisellini 2008).

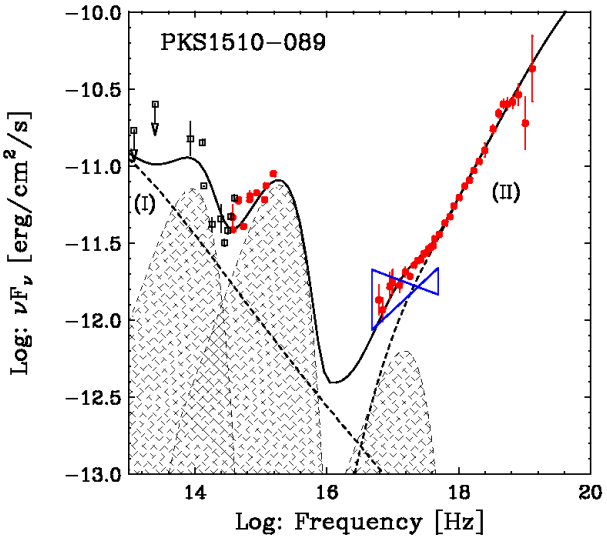

Fig. 5. The IR-to-hard X-ray spectrum of PKS 1510–089 during the *Suzaku* 2006 August campaign. The left hump mimics excess emission from the dusty torus, whereas the middle hump mimics the accretion disk emission, and the right hump shows the best-fit blackbody-type emission of $kT \approx 0.2$ keV from the *Suzaku* fitting. The dotted lines show (I) the synchrotron and (II) the inverse–Compton components, respectively. The solid line shows the sum of all the model components. *(from Kataoka et al. 2008.)*

3. Future Perspectives: X-ray Polarimetry

Polarization of blazar synchrotron emission is now routinely detected at radio and optical frequencies, with the polarization degree and polarization angle depending on frequency and the activity level of a source. These new observations allowed for a novel insight into the internal structure and magnetic field topology of AGN jets (see, e.g., Marscher et al., 2008; Abdo et al., 2010). The detection of the X-ray polarization of blazar sources would be therefore of a primary importance. The Soft Gamma-ray Detector (SGD) onboard the ASTRO-H satellite, to be launched in 2015, is designed for the spectroscopy and high-precision polarimetry within the hard X-ray/soft γ-ray range 50–600 keV (Tajima et al. 2010, Watanabe et al. 2012). Among several targets bright enough in this band, including Crab pulsar and nebulae, or Galactic microquasars such as Cyg X-1, flaring BL Lacs with hard X-ray spectra dominated by the synchrotron jet emission constitute an another class of promising targets for the X-ray polarimetry with SGD. Note in this context that during the April 1997 outburst of the BL Lac object Mrk 501 the flat-spectrum synchrotron component extended up to ≥ 100 keV photon energies, with the persistent (over several days) flux of about ~ 100 mCrab (Pian et al. 1998).

The X-ray continua of luminous FSRQ, as mentioned in the previous section, are dominated by the inverse-Compton emission of the lowest-energy jet electrons. Interestingly, the inverse-Compton emission can also be polarized at some level, with the polarization degree depending on polarization properties of soft target photons, or on the geometry of the emitting region and the jet bulk velocity (McNamara et al. 2009, Krawczynski 2012, Zhang & Boettcher 2013). Model predictions indicate in particular that the synchrotron self-Compton emission of blazar sources may be polarized up to even 40%. Hence, the SGD observations of FSRQs may in principle provide interesting constraints on the blazar emission models as well.

References

Abdo, A. A., et al. 2010, Nature, 463, 919
Ackermann, M., et al. 2012, Science, 338, 1190
Anderhub, H., et al. 2009, ApJ, 705, 1624
Asano, K., et al.. 2014, ApJ, 780, 64
Blandford, R. D., & Koenigl, A. 1979, ApJ, 232, 34
Boutelier, T., et al. 2008, MNRAS, 390, L73
Cao, G., & Wang, J. 2013, PASJ, 65, 109
Celotti, A., & Ghisellini, G. 2008, MNRAS, 385, 283
Celotti, A., et al. 2007, MNRAS, 375, 417
Dermer, C. D. & Schlickeiser, R. 1993, ApJ, 416, 458
Dermer, C. D., et al. 2011, ApJL, 733, L21
Finke, J. D., et al. 2008, ApJ, 686, 181
Fossati, G., et al. 2008, ApJ, 677, 906
Ghisellini, G. 2013, European Physical Journal Web of Conferences, 61, 5001
Ghisellini, G., et al. 2010, MNRAS, 405, 387
Hayashida, M., et al. 2012, ApJ, 754, 114
Isobe, N., et al. 2010, PASJ, 62, L55
Kataoka, J., et al. 2001, Apj, 560, 659
Kataoka, J., et al. 2008, ApJ, 672, 787
Katarzynski, K., et al. 2006, A&A, 453, 47
Kokubun, M., et al. 2007, PASJ, 59, 53
Koyama, K., et al. 2007, PASJ, 59, 23
Krawczynski, H. 2012, ApJ, 744, 30
Lanzuisi, G., et al. 2012, MNRAS, 421, 390
Marscher, A. P. & Gear, W. K. 1985, ApJ, 298, 114
Marscher, A. P., et al. 2008, Nature, 452, 966
McNamara, A. L., et al. 2009, MNRAS, 395, 1507
Mitsuda, K., et al. 2007, PASJ, 59, 1
Moderski, R., et al. 2004, ApJ, 611, 770
Neronov, A., & Vovk, I. 2010, Science, 328, 73
Pian, E., et al. 1998, ApJL, 492, L17
Poutanen, J., & Stern, B. 2010, ApJL, 717, L118
Reimer, A., et al. 2008, ApJ, 682, 775
Sauge, L., & Henri, G. 2004, ApJ, 616, 136
Sbarrato, T., et al. 2012, MNRAS, 421, 1764
Sikora, M., & Madejski, G. 2000, ApJ, 534, 109
Sikora, M., et al. 1994, ApJ, 421, 153
Sikora, M., et al. 2009, ApJ, 704, 38
Sikora, M., et al. 2013, ApJ, 779, 68
Stawarz, Ł., & Petrosian, V. 2008, ApJ, 681, 1725

Tagliaferri, G., et al. 2008, ApJ, 679, 1029
Tajima, H. et al., 2010, Proc. SPIE, 7732, 773216
Takahashi, T., et al. 2000, ApJL, 542, L105
Takahashi, T., et al. 2007, PASJ, 59, 35
Tanaka, T., et al. 2008, ApJ, 685, 988
Tanaka, Y.T., et al. 2014, ApJ, 787, 155
Tavecchio, F., et al. 2010, MNRAS, 401, 1570
Tavecchio, F., et al. 2011, MNRAS, 414, 3566
Tramacere, A., et al. 2009, A&A, 501, 879
Ushio, M., et al. 2009, ApJ, 699, 1964
Ushio, M., et al. 2010, ApJ, 724, 1509
Watanabe, S., et al. 2009, ApJ, 694, 294
Watanabe, S., et al., 2012, Proc. SPIE, 8443, 844326
Zhang, H., & Boettcher, M. 2013, ApJ, 774, 18